Contents lists available at ScienceDirect

Digital Chinese Medicine

journal homepage: http://www.keaipublishing.com/dcmed

Niuhuang (Bovis Calculus)-Shexiang (Moschus) combination induces apoptosis and inhibits proliferation in hepatocellular carcinoma via PI3K/AKT/mTOR pathway

NING Dimin[a], DENG Zhe[a], WU Yongrong[a], MEI Si[b], TENG Yongjie[c], ZHOU Qing[c], TIAN Xuefei[a]*

a. Hunan Key Laboratory of Translational Research in Formulas and Zheng of Traditional Chinese Medicine, College of Integrated Traditional Chinese and Western Medicine, Hunan University of Chinese Medicine, Changsha, Hunan 410208, China

b. Department of Physiology, Hunan University of Chinese Medicine, Changsha, Hunan 410208, China

c. Department of Andrology, The First Hospital of Hunan University of Chinese Medicine, Changsha, Hunan 410007, China

ARTICLE INFO

Article history
Received 02 November 2021
Accepted 20 December 2021
Available online 25 March 2022

Keywords
Niuhuang (Bovis Calculus)
Shexiang (Moschus)
Hepatocellular carcinoma
PI3K/AKT/mTOR singnaling pathway
Caspase-3
Caspase-9
Bcl-2
Bax
Cell apoptosis

ABSTRACT

Objective To investigate the effects of Niuhuang (Bovis Calculus, BC) and Shexiang (Moschus) (BC-Moschus) on human hepatocellular carcinoma (HCC) cells SMMC-7721 and a nude mouse model of subcutaneous xenografts, and to explore its anti-HCC mechanism.

Methods The BC-Moschus combination was applied to two liver cancer models *in vivo* and *in vitro*. SMMC-7721 was divided into the BC-Moschus group and the control group, and different doses (rude drug dosage 0.625, 1.25, 2.5, and 5 mg/mL) of BC-Moschus extract were used for the intervention. The proliferation ability of HCC cells was detected using the Cell Counting Kit-8 (CCK-8) assay, and the migration ability was detected by a wound healing assay. A subcutaneous xenograft model was prepared using nude mice with human HCC. Specific pathogen-free-grade BALB/c nude mice (5-week-old) were randomly divided into the following groups (n = 6 per group): control (0.9% physiological saline 0.2 mL/d), BC-Moschus [BC 45.5 mg/(kg·d) + Moschus 13 mg/(kg·d)], and cisplatin (DDP, intraperitoneal injection 5 mg/kg per week) groups. All groups were administered for 14 d. The volume and mass of the subcutaneous xenografts in nude mice were observed. The expression levels of phosphatidylinositol-3 kinase/protein kinase B/mammalian target of rapamycin (PI3K/AKT/mTOR) pathway, apoptosis-associated factor p70 S6 Kinase (S6K), Bax, Bcl-2, caspase-3, and caspase-9 in nude mice subcutaneous xenografts were measured by real-time quantitative PCR (RT-qPCR) and Western blot. Terminal Deoxynucleotidy Transferase-Mediated dUTP Nick-End Labeling (TUNEL) was used for quantitative analysis of apoptotic cells.

Results The CCK-8 assay demonstrated that the BC-Moschus combination inhibited HCC cell proliferation in a superior manner to the use of BC and Moschus alone, and the inhibition effect was dose- and time-dependent ($P < 0.01$). The wound healing assay showed that the BC-Moschus combination inhibited HCC cell migration ($P < 0.01$). In the subcutaneous xenograft model of nude mice with human HCC, we found that the tumor volume and weight of the BC-Moschus group were lower than those of the control group ($P < 0.01$). The levels of the PI3K/AKT/mTOR signaling pathway and S6K protein in the BC-Moschus and DDP groups were significantly decreased ($P < 0.01$). The expression level of the anti-apoptotic gene Bcl-2 was downregulated ($P < 0.05$), and the expression of the pro-apoptotic gene Bax

*Corresponding author: TIAN Xuefei, Professor, E-mail: 003640@hnucm.edu.cn.

Peer review under the responsibility of Hunan University of Chinese Medicine.

DOI: 10.1016/j.dcmed.2022.03.009

Citation: NING DM, DENG Z, WU YR, et al. Niuhuang (Bovis Calculus)-Shexiang (Moschus) combination induces apoptosis and inhibits proliferation in hepatocellular carcinoma via PI3K/AKT/mTOR pathway. Digital Chinese Medicine, 2022, 5(1): 83–92.

and apoptosis-related factors caspase-3 and caspase-9 were significantly upregulated ($P < 0.01$). The TUNEL assays further confirmed that the combination of the BC-Moschuas could promote HCC ($P < 0.01$).

Conclusion The BC-Moschus combination inhibited the proliferation and migration ability of HCC cells SMMC-7721 and effectively inhibited the growth of subcutaneous xenografts in nude mice. The mechanism may be closely related to the downregulation of the PI3K/AKT/mTOR pathway, regulation of apoptosis-related protein caspase-3, caspase-9, Bcl-2, and Bax expression, and promotion of apoptosis.

1 Introduction

Hepatocellular carcinoma (HCC) is the most common type of primary liver cancer and is an aggressive tumor with a poor prognosis [1, 2]. In recent years, dysregulation of various molecular mechanisms has been shown to contribute to the pathogenesis of HCC [3]. The phosphatidylinositol 3-kinase/protein kinase B/mammalian target of rapamycin (PI3K/AKT/mTOR) signaling system, which controls multiple crucial cellular processes such as cell proliferation, survival regulation, and metabolism, is the most critical and over-activated pathway in approximately 50% of HCC [4-6]. The second messenger produced by activated PI3K binds to and phosphorylates the serine-threonine kinase AKT [7]. AKT then stimulates mTOR via phosphorylation, which in turn regulates its downstream protein p70 S6 kinase (S6K) via phosphorylation of S6K (p-S6K), inhibiting the production of pro-apoptotic protein Bax while promoting the expression of anti-apoptotic protein Bcl-2 family members. Moreover, the Bcl-2 family suppresses cytochrome C release and activation of cleaved caspase-9 and cleaved caspase-3 [8]. Resultingly, targeted suppression of the PI3K/AKT/mTOR signaling pathway represents a viable therapeutic option for HCC.

Niuhuang (Bovis Calculus, BC) and Shexiang (Moschus) are precious animal durgs that are widely used to treat various ailments [9-12]. BC is derived from dried gallstones removed from the gallbladder or bile duct of domestic cattle and possesses anti-inflammatory, antipyretic, detoxifying, sedative, and gallbladder function recovery properties [11]. BC has anti-tumor properties and has been found to reduce the proliferation of mouse malignant sarcoma cells S180, with the mechanism being linked to the activity of the PI3K/AKT pathway [12]. HCC cells are subjected to natural moschus and synthetic muskone, which can cause growth inhibition and apoptosis [13], and muskone can activate the PI3K/AKT signaling pathway [12]. However, the specific role and mechanism of the BC-Moschus combination in HCC treatment are currently unclarified. In this study, the BC-Moschus combination was used to study the effects and mechanisms of the two in HCC.

2 Materials and methods

2.1 Reagents

BC (Hunan Sanxiang Traditional Chinese Medicine Yinpian Co., Ltd., China), Moschus (Lhasa Changdu Chinese Medicine Yinpian Factory, China), cisplatin (DDP, Beijing Solebo Technology Co., Ltd., China), Fetal Bovine Serum (FBS, Gibco, USA), penicillin-streptomycin (Gibco, USA), Cell Counting Kit-8 (CCK-8, Gibco, USA), Teminal Deoxynucleotidy Transferase Mediated dUTP Nick-End Labeling (TUNEL) kit (Jiangsu KGI Biotechnology Co., Ltd., China), Bicinchoninic Acid (BCA) kit (Beyotime, China), TRIzol reagent (Invitrogen, USA), PrimeScriptTM RT Master Mix (Takara, China), SYBR Green (Takara, China). Antibodies against PI3K, Bax, Bcl-2 and β-actin were obtained from Proteintech Group, Inc. (USA). Phosphorylated (p)-PI3K, AKT, p-AKT, mTOR, p-mTOR, cleaved caspase-3, cleaved caspase-9, and p-S6K were obtained from Abcam (UK). For *in vitro* studies, BC and Moschus were dissolved in dimethyl sulfoxide (DMSO, Sigma-Aldrich, China), and were added to the culture medium at the indicated concentrations of 0.625, 1.25, 2.5, and 5 mg/mL, respectively. The DMSO concentration was maintained at < 0.5%. For *in vivo* studies, BC and Moschus were ground into powder and dissolved in 0.9% isotonic sodium chloride solution for intragastric administration. According to the *Chinese Pharmacopoeia* (2015 edition), the BC and Moschus doses for adults were 0.35 and 0.10 g/d, respectively. According to the equivalent dose conversion between humans and mice, the BC and Moschus doses were 45.5 and 13.0 mg/(kg·d), respectively. The clinically equivalent dose of DDP was 5 mg/kg [14, 15].

2.2 Cell culture

The HCC cell line SMMC-7721 was identified by short tandem repeat (Beijing Nortel Biotechnology Institute, China), which was cultivated in Dulbecco's Modified Eagle Medium (DMEM) supplemented with 10% heat-inactivated FBS and 1% penicillin-streptomycin. The cells were incubated in a 5% CO_2 incubator at 37 °C.

2.3 Cell viability assay

The cell inhibition rate was assessed using the CCK-8. SMMC-7721 cells at the logarithmic growth stage were digested and counted using a hemocytometer. Cells (5×10^3 cells per well) were seeded and cultured in 96-well microplates. The groups were divided into BC-Moschus, BC, Moschus, and control groups. Six multiple wells were set up for each group and treated with different doses for 48 h. When the cells had achieved 90% confluence, 10 μL of the CCK-8 reagent was added to each well. The cells were cultured for 2 h at 37 °C with 5% CO_2, after which the absorbance optical density (OD) value at 450 nm was measured with a microplate analyzer, and the half-limiting dose (IC_{50}) was calculated to determine the SMMC-7721 cell proliferation activity in each group.

2.4 Wound-healing assay

A total of 3×10^5 cells were seeded in each well of a 6-well plate. After the cells reached 100% confluence, scratches were made using a 100 μL tip, and cell debris was washed away with phosphate-buffered saline. Next, serum-free medium containing 5 mg/mL BC-Moschus was added and the plates were cultured in an incubator. Representative images were taken at 12, 24, and 48 h using an optical microscope at 40× magnification. Image J software was used to calculate the cell scratch area, and cell mobility = (12 h scratch area – scratch area after culture)/12 h scratch area × 100%.

2.5 Animal and tumor xenotransplantation studies

In this study, specific pathogen-free (SPF)-grade pure BALB/c nude mice were used. The mice (5-week-old and 20 g, n =18) were purchased from Hunan Silaike Jingda Laboratory Animal Co., Ltd. (Changsha, China; laboratory animal quality certificate No. 11072719110019711; laboratory facilities certificate No. SCXK [Xiang] 2015-0017). All animals were maintained under SPF conditions. A subcutaneous xenograft model was performed in nude mice using the method proposed by HOU et al. [16]. SMMC-7721 cells (1×10^7) were subcutaneously injected into the nude mice to form subcutaneous xenograft tumors. When the tumor volume reached approximately 100 mm^3, mice were randomly divided into three treatment groups of six mice each: control (0.9% normal saline 0.2 mL/d by gavage), BC-Moschus [BC 45.5 mg/(kg·d) + Moschus 13 mg/(kg·d) by gavage], and DDP (weekly intraperitoneal injection of DDP 5 mg/kg). The volume and body weight of the nude mice were measured every two days during the 14 d treatment period. The tumor volume was calculated as the maximum tumor length × width^2 × 0.5. After 14 d of treatment, the mice were euthanized for cervical dislocation according to the Animal Research: Reporting of *In Vivo* Experiments (ARRIVE) Guidelines, and the subcutaneous graft tumors were aseptically excised, weighed, and photographed for documentation. The tumor tissue samples were stored at – 80 °C in a 4% paraformaldehyde solution for pathological examination. All animals were carefully cared for, and the experiments were approved by the Experimental Animal Welfare Ethics Review Committee of Central South University (Approval No. 20198 YDW3579).

2.6 TUNEL assay

The tumor tissue samples were cut into 5 mm × 5 mm blocks, dehydrated, waxed, embedded, sectioned, and stained according to the standard protocol. Tumor tissue samples apoptosis were detected by fluorescence microscopy in strict accordance with the TUNEL kit. Nuclei and apoptotic cells were fluoresced in blue and red, respectively. Three areas of each tissue sample section were randomly selected, and the number of apoptotic cells was counted.

2.7 Western blot analysis of proteins associated with PI3K/AKT/mTOR signaling pathway and apoptosis

A total of 25 mg of mouse tumor tissue samples were used to prepare the protein lysates. After pre-cooling and washing, 300 μL RIPA lysate was added for lysis for 10 min, centrifuged at 12 000 RCF at 4 °C for 10 min, and then the supernatant was retrieved. Protein concentration was quantified using a BCA kit. After boiling, the samples were loaded onto SDS PAGE gels with 2 μL marker in the first well and 50 μL of lysate in each well. Electrophoresis was performed at a constant voltage of 75 V for 130 min. The protein samples were separated by electrophoresis and transferred onto polyvinylidene fluoride membranes, which were then blocked with 5% skim milk at 37 °C for 60 min. The membranes were incubated with the primary antibody at 4 °C overnight and washed with 1 × PBST after incubation. Secondary antibodies were added, and the membranes were incubated at room temperature for 60 min and then washed with 1 × PBST. Protein expression was visualized using an enhanced chemiluminescence reagent, and the membrane images were captured using a BOX Chemi XRQ imaging system (SynGene, UK). The following primary antibodies were used: antibodies against PI3K (1∶5 000), Bax (1∶6 000), Bcl-2 (1∶2 000), and β-actin (1∶5 000), phosphorylated (p)-PI3K (1∶2 000), AKT (1∶2 000), p-AKT (1∶2 000), mTOR (1∶2 000), p-mTOR (1∶2 000), cleaved caspase-3 (1∶4 000), cleaved caspase-9 (1∶2 000), and p-S6K (1∶1 000).

2.8 Real-time quantitative PCR (RT-qPCR)

Total RNA was extracted from tumor tissue samples in each group using TRIzol reagent according to the manufacturer's instructions. Total RNA was reverse transcribed into cDNA using PrimeScriptTM RT Master Mix, and the resulting cDNA was used as a template for

RT-qPCR amplification. Positive/negative primer pairs were used for the tested genes using. Three separate amplifications were performed using the ABI StepOne Plus system (Applied Biosystems, USA). The forward and reverse primers used are listed in Table 1.

Table 1 Primer sequences of RT-qPCR

Gene	Upstream primer	Downstream primer
PI3K	5'-CGAGAGTGTCGT CACAGTGTC-3'	5'-GACACAAACAC CTTCGCTTGT-3'
AKT	5'-CCCTGCTCCTA GTCCACCA-3'	5'-CTCGGGTGACTT TGTCTCTGT-3'
mTOR	5'-CCGCTACTGTGT CTTGGCAT-3'	5'-AGAAACTCTAG GCGCTCGAC-3'
Bcl-2	5'-TTGAAAACCGAAC CAGGAATTGC-3'	5'-TCTCGTTCACCG TGTCCTG-3'
Bax	5'-TGAAGACAGGG GCCTTTTTG-3'	5'-GCTGACAGAGG CCGCTTAA-3'
p-S6K	5'-TGCTAAGGACAC GGCCCACA-3'	5'-ACACCTGGACTA AATACGGAAA-3'
Caspase-3	5'-TCTGACTGGAAA GCCGAAACTCT-3'	5'-ACCCTGACTA CTCCTCTACCGA-3'
Caspase-9	5'-GGCTGTTAAAC CCCTAGACCA-3'	5'-ATCACTTCGA CCTGGGCAGT-3'
β-Actin	5'-FACATCCGTAAAG ACCTCTATGCC-3'	5'-CACCTAGTCGTT CGTCCTCAT-3'

2.9 Statistical analysis

All statistical calculations were performed using the statistical software GraphPad Prism 7 (GraphPad Software, USA). Data are presented as the mean ± standard deviation (SD). One-way analysis of variance followed by the least significant difference test or Student's *t* test was used to determine significance. Statistical significance was set at $P < 0.05$.

3 Results

3.1 Inhibitory effects of the BC-Moschus combination on HCC cell proliferation and migration

The results showed that the BC-Moschus combination inhibited HCC cell proliferation in a superior manner to the use of BC and Moschus alone (Figure 1A); the BC-Moschus combination had an inhibitory effect on HCC cells in a dose- and time-dependent manner (Figure 1B). Furthermore, we tested the effects of the BC-Moschus combination on HCC cell migration using a wound healing assay. The results showed that the mean cell migration rates at 24 and 48 h were 55.8% and 94.7% in the control group, 21.5% and 57% in the BC-Moschus group, and 9% and 45.5% in the DDP group, respectively ($P < 0.01$, Figure 1C). Therefore, the cell migration rate was significantly reduced in the BC-Moschus and DDP groups compared with that in the control group ($P < 0.01$), indicating that BC-Moschus and DDP inhibited HCC cell migration.

3.2 Effects of BC-Moschus on subcutaneous xenograft tumors of HCC in nude mice

Compared with that of the control group, the tumor size was reduced in the BC-Moschus and DDP groups ($P < 0.01$, Figure 2A), and the tumor volume was decreased ($P < 0.01$, Figure 2B). Meanwhile, the tumor weight of the BC-Moschus and DDP groups was significantly lower than that of the control group ($P < 0.01$, Figure 2C). Furthermore, there was no significant change in the body weight of mice in either group ($P > 0.05$, Figure 2D). Therefore, the BC-Moschus group could inhibit the volume and weight increase of subcutaneous xenograft tumors in nude mice.

3.3 Effects of the BC-Moschus on the expression of the PI3K/AKT/mTOR pathway

The protein to phosphorylation ratio of the PI3K signaling pathway demonstrated that, in the BC-Moschus and DDP groups, the p-PI3K/PI3K ratio was significantly lower than that in the control group ($P < 0.01$). The p-AKT/AKT ratio showed that the BC-Moschus and DDP groups decreased compared with the control group ($P < 0.01$). Meanwhile, the p-mTOR/mTOR ratio showed that, compared with that of the control group, the ratio of the BC-Moschus group to the DDP group was decreased ($P < 0.01$). Moreover, compared with that of the BC-Moschus group, the ratio of the DDP group was decreased ($P < 0.01$, Figure 3A). The mRNA expression of the PI3K/AKT/mTOR signaling pathway showed that PI3K expression in the BC-Moschus and DPP groups was significantly decreased compared with that in the control group ($P < 0.01$), while that in the DDP group was increased compared with that in the BC-Moschus group ($P < 0.01$). Meanwhile, the mRNA AKT expression showed the same trend as that of PI3K ($P < 0.01$). The mRNA mTOR expression in the BC-Moschus group was lower than that in the control group, while the expression increased in the DDP group compared to that in the BC-Moschus group ($P < 0.01$, Figure 3B). In addition, we detected the expression of apoptosis-related genes downstream of the PI3K/AKT/mTOR pathway. The results showed that, compared with that of the control group, the protein expression of the pro-apoptotic gene Bax increased in the BC-Moschus and DDP groups ($P < 0.01$). The protein expression of the anti-apoptotic gene Bcl-2 was decreased in the BC-Moschus and DDP groups compared with that in the control group ($P < 0.05$ and $P < 0.01$, respectively). Meanwhile, Bcl-2 expression in the DDP group was lower than that in the BC-Moschus group ($P < 0.01$). In addition, the

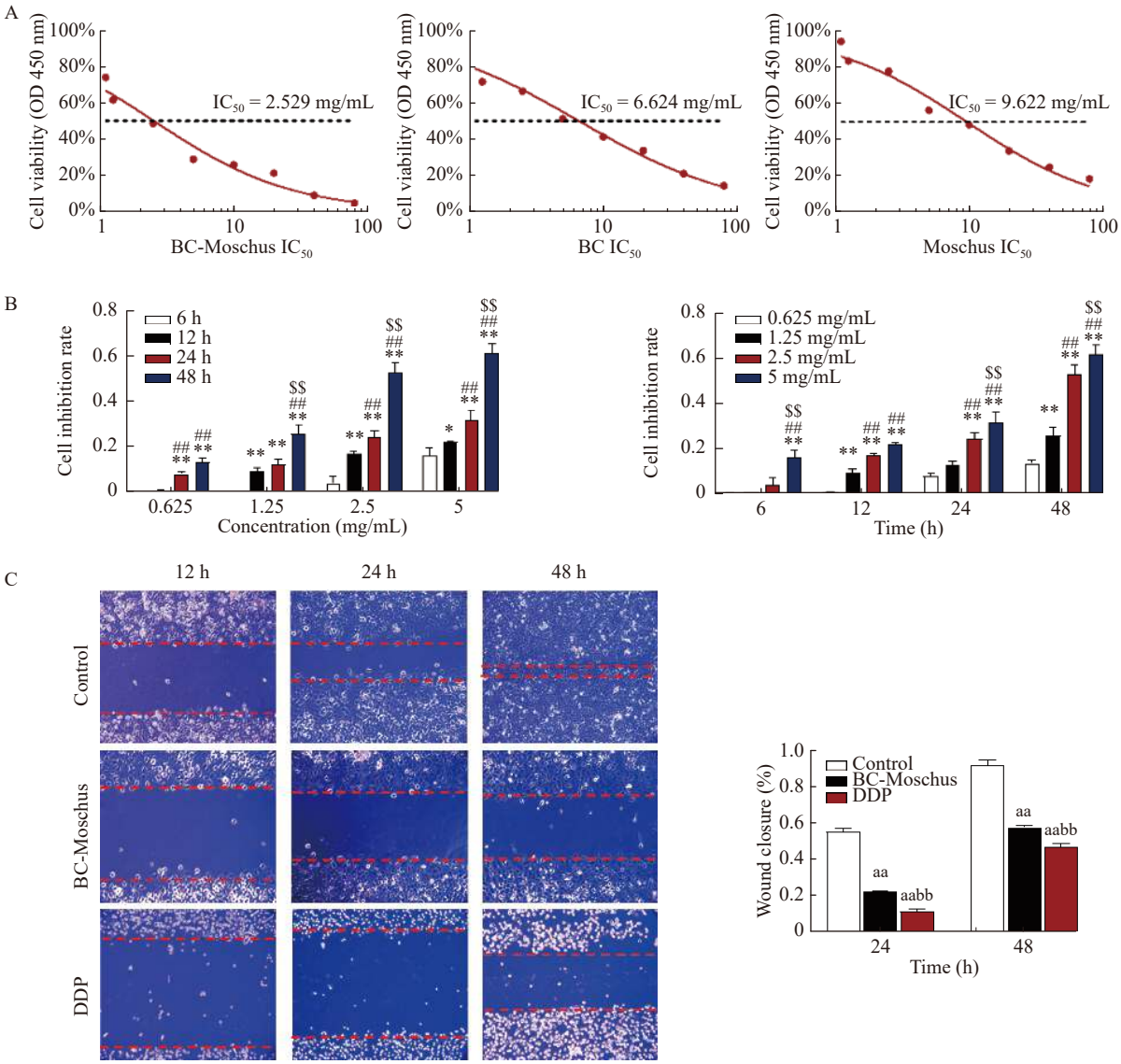

Figure 1 HCC cell proliferation and migration following BC-Moschus combination treatment

A, determination of IC_{50} in BC-Moschus, BC, and Moschus groups. B, cell viability was assessed using the CCK-8 assay. C, cell migration ability in different groups detected by the wound healing assay. Data are expressed as the mean ± SD. $^{*}P < 0.05$, $^{**}P < 0.01$, compared with 6 h (0.625 mg/mL); $^{\#\#}P < 0.01$, compared with 12 h (1.25 mg/mL); $^{\$\$}P < 0.01$, compared with 24 h (2.5 mg/mL); $^{aa}P < 0.01$, compared with the control group; $^{bb}P < 0.01$, compared with the BC-Moschus group.

phosphorylated S6K protein decreased in the BC-Moschus and DDP groups ($P < 0.01$, Figure 3C). Furthermore, Bax, Bcl-2, and S6K mRNA expression showed a consistent trend with protein expression ($P < 0.01$, Figure 3D). In conclusion, our results suggest that the BC-Moschus can inhibit PI3K/AKT/mTOR and its downstream apoptosis-related signaling pathways.

3.4 Effects of the BC-Moschus combination on HCC cell apoptosis

The results showed that, compared with that of the control group, cleaved caspase-3 protein expression in the BC-Moschus and DDP groups was not statistically significant ($P > 0.05$). The cleaved caspase-9 protein expression was increased in the BC-Moschus and DDP groups compared to that in the control group ($P < 0.05$ and $P < 0.01$, respectively), and the expression was increased in the DDP group compared to that in the BC-Moschus group ($P < 0.01$, Figure 4A). The mRNA expression results showed that caspase-3 and caspase-9 expression was significantly increased in the BC-Moschus group compared with that in the control group ($P < 0.01$), while caspase-3 and caspase-9 expression was lower in the DDP group than that in the BC-Moschus group ($P < 0.01$, Figure 4B). In addition, the TUNEL assay was used to detect the number of apoptotic cells in subcutaneous xenograft tumors of nude mice in each group. The results showed that the number of apoptotic cells in the BC-Moschus and DDP groups were higher than that in the control group ($P < 0.01$, Figure 4C). In conclusion, the results showed that the BC-Moschus combination upregulated the expression of apoptosis executors and promoted HCC cell apoptosis.

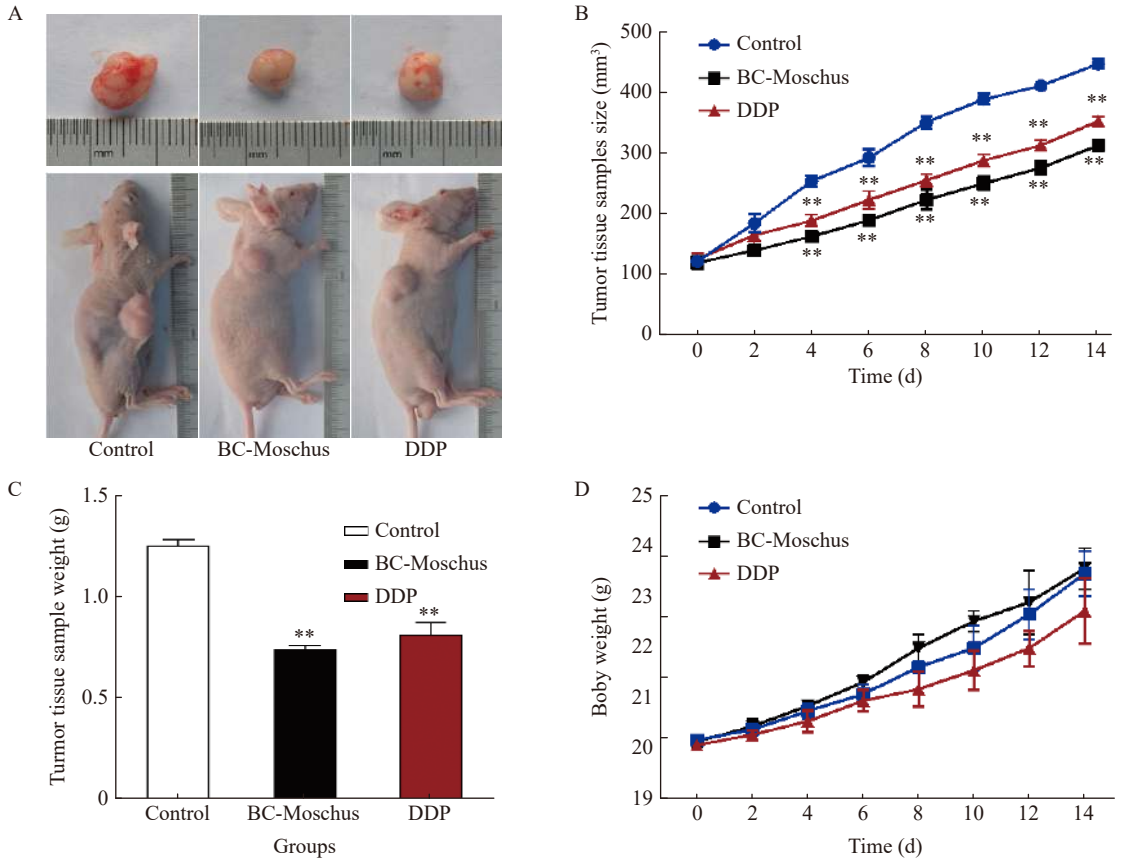

Figure 2 Inhibitory effects of the BC-Moschus combination on subcutaneous xenograft tumors of HCC in nude mice

A, representative tumor image at the end of the treatment. B, mean subcutaneous xenograft tumor volume. C, subcutaneous xenograft tumor weight in each group. D, average body weight of the mice during treatment. Data are expressed as the mean ± SD. $^{**}P < 0.01$, compared with the control group.

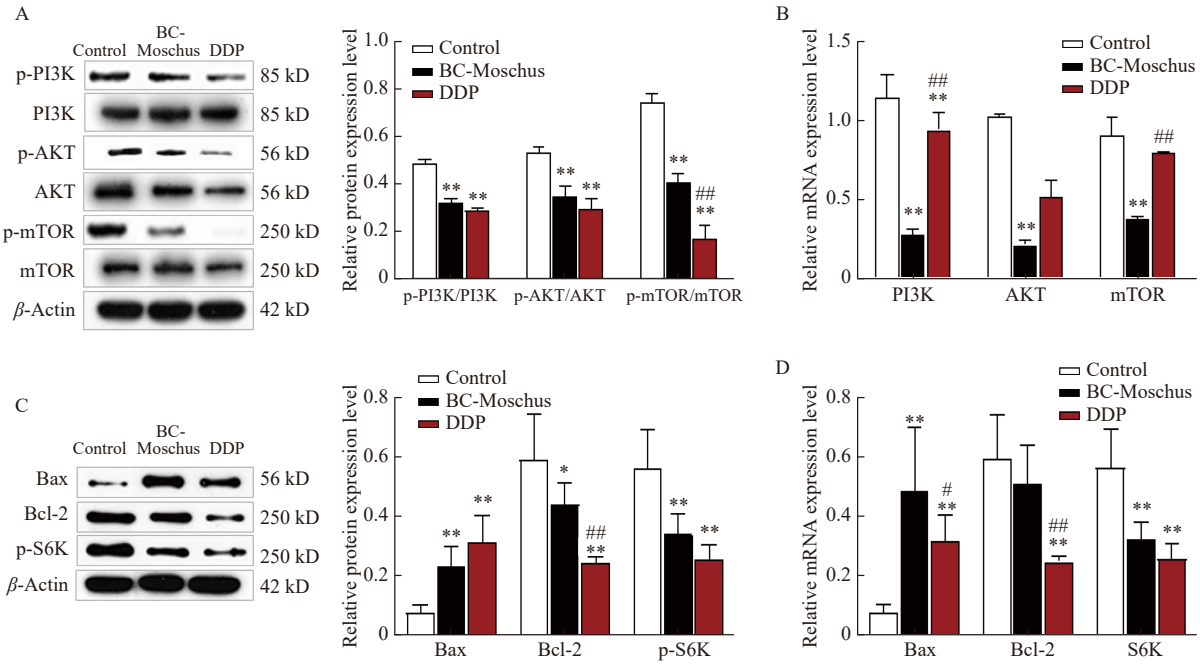

Figure 3 The expression levels of PI3K/AKT/mTOR pathway and downstream apoptosis-related genes after treatment in each group

A and B, protein and mRNA expression of the PI3K/AKT/mTOR pathway in each group. C and D, the protein and mRNA expression of Bax, Bcl-2, and p-S6K in each group. Data are expressed as the mean ± SD. $^{*}P < 0.05$, $^{**}P < 0.01$, compared with the control group; $^{\#}P < 0.05$, $^{\#\#}P < 0.01$, compared with the BC-Moschus group.

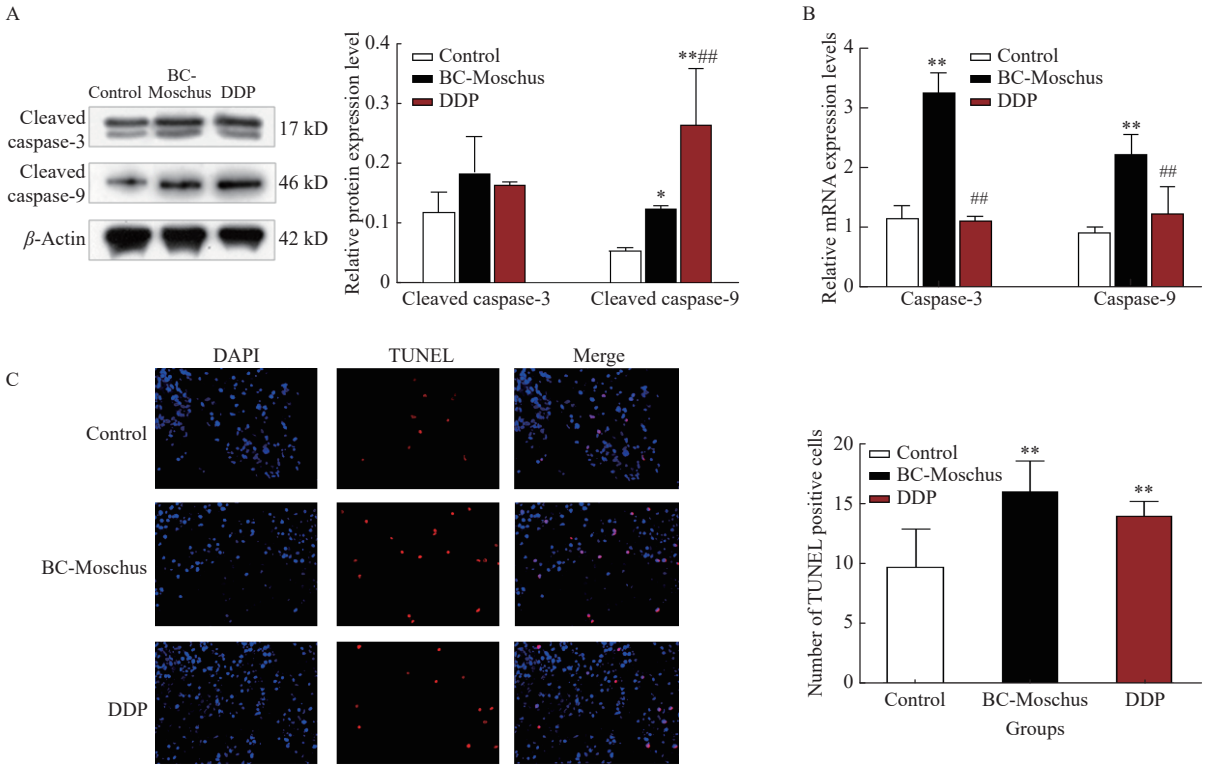

Figure 4 Effects of the BC-Moschus combination on HCC cell apoptosis

A, protein expression of cleaved caspase-3 and cleaved caspase-9 in each group. B, mRNA expression of caspase-3 and caspase-9 in each group. C, the number of apoptotic cells in subcutaneous xenograft tumors in each group (40 ×). Data are presented as mean ± SD. $^{*}P < 0.05$, $^{**}P < 0.01$, compared with the control group; $^{\#\#}P < 0.01$, compared with the BC-Moschus group.

4 Discussion

HCC is the main type of primary liver cancer with high morbidity and mortality worldwide [17]. According to the World Health Organization (WHO) statistics, by 2030, more than one million patients will have died of liver cancer [18, 19]. Oxidative stress, apoptosis, cholestasis, and bile acid disorders play important roles in the HCC development [20-23]. BC and Moschus have been used as traditional Chinese animal-derived therapeutic drugs for more than 2 000 years in China. BC can improve intrahepatic cholestasis, restore bile acid homeostasis, and protect the liver through the signal transduction pathway mediated by the farnesoid X receptor [24, 25]. Moreover, BC promotes HepG2 cell apoptosis [26]. Meanwhile, through data mining of network pharmacology, we showed that the effects of BC on primary liver cancer were predominantly focused on apoptosis and the PI3K-AKT signaling pathway, and the molecular targets with multiple intersections were apoptosis executor factors such as cleaved caspase-3 and cleaved caspase-9 [27]. Recently, the antitumor activity of Moschus has gradually been revealed. Both natural and synthetic Moschus induce growth inhibition and apoptosis in numerous neoplastic diseases, and their therapeutic effects are dose-dependent [13]. QI et al. [28] reported that muskone played an anticancer role by inducing HCC cell apoptosis and autophagy. Xihuang Pill (西黄丸, XHP), a traditional Chinese medicine compound with BC and Moschus as the main components, has also been used in liver cancer treatment [29-32], however, the mechanism of action on liver cancer remains unclear.

The PI3K pathway can provide basic metabolites through glycolysis and adipogenesis, and promote cancer cell growth [33]. AKT is associated with resistance to malignant transformation and apoptosis [7]. The survival of continuously active tumor cells may depend on AKT [34, 35]. mTOR is a kinase downstream of AKT, which is phosphorylated by the PI3K/AKT pathway [36, 37]. The PI3K/AKT/mTOR signaling pathway is the most common hyperactivated signaling pathway in HCC [38], and it has become an attractive target for HCC treatment by regulating multiple processes, such as the cell cycle, apoptosis, and metabolism [39-42]. Our findings showed that the BC-Moschus combination inhibited HCC cell proliferation and migration *in vitro*, and also confirmed that the BC-Moschus combination could inhibit the growth of subcutaneous xenograft tumors in nude mice *in vivo*. We further explored the mechanism of HCC inhibition by the BC-Moschus combination, and determined that the BC-Moschus combination could effectively inhibit the expression of members of the PI3K/AKT/mTOR signaling pathway. Thus, based on these findings, it can be inferred that the BC-Moschus combination inhibits HCC by inhibiting the PI3K/AKT/mTOR signaling pathway.

It has been reported that simultaneous inhibition of the PI3K/AKT/mTOR pathway and Bcl-2/Bcl-xL can

increase apoptosis [43, 44]. mTOR induces phosphorylation of its downstream protein, S6K, which in turn regulates the Bcl-2/Bcl-xL apoptosis pathway. The Bcl-2 protein family plays a key role in apoptosis through the mitochondrial pathway [45] and inhibits the Bcl-2 protein by activating a member of the BH3-only family (promoter), thereby activating the pro-apoptotic effector Bax [46]. Activated Bax then penetrates the outer membrane of mitochondria, causing cytochrome C to be released into the cytoplasm. Released cytochrome C promotes caspase-9 activation, which in turn activates the apoptotic effector protein caspase-3. Caspase-3 is the primary executor of apoptosis, which can specifically cleave substrates such as PARP, eventually leading to DNA breakage and cell apoptosis [46, 47]. Our results indicated that the BC-Moschus combination inhibited the PI3K/AKT/mTOR signaling pathway, downregulated p-S6K expression, and inhibited the expression of the anti-apoptotic gene Bcl-2. Moreover, the pro-apoptotic gene Bax cleaved caspase-9, and cleaved caspase-3 expression was promoted. Simultaneously, we detected the apoptosis of subcutaneous xenograft tumors in nude mice, and the results confirmed that the BC-Moschus combination can promote HCC cell apoptosis.

5 Conclusion

In this study, we demonstrates that the BC-Moschus combination can promote apoptosis by inhibiting the PI3K/AKT/mTOR pathway, and it plays a role in reducing the proliferation, migration, and growth of HCC. This study revealed the anti-HCC effect and mechanism of the BC-Moschus combination to a certain extent, providing evidence for future clinical applications and basic research.

Fundings

National Natural Science Foundation of China (81473617), Natural Science Foundation of Hunan Province (2020JJ4066), Scientific Research Project of Hunan Education Department (18A266), and Hunan Graduate Scientific Research Innovation Project (QL20210173).

Competing interests

The authors declare no conflict of interest.

References

[1] ANWANWAN D, SINGH SK, SINGH S, et al. Challenges in liver cancer and possible treatment approaches. Biochimica Et Biophysica Acta-Reviews on Cancer, 2020, 1873(1): 188314.

[2] CRAIG AJ, VON FELDEN J, GARCIA-LEZANA T, et al. Tumour evolution in hepatocellular carcinoma. Nature Reviews Gastroenterology Hepatology, 2020, 17(3): 139–152.

[3] OGUNWOBI OO, HARRICHARRAN T, HUAMAN J, et al. Mechanisms of hepatocellular carcinoma progression. World Journal of Gastroenterology, 2019, 25(19): 2279–2293.

[4] ENGELMAN JA. Targeting PI3K signalling in cancer: opportunities, challenges and limitations. Nature Reviews Cancer, 2009, 9(8): 550–562.

[5] KHEMLINA G, IKEDA S, KURZROCK R. The biology of hepatocellular carcinoma: implications for genomic and immune therapies. Molecular Cancer, 2017, 16(1): 149.

[6] KIM J, JUNG KH, RYU HW, et al. Apoptotic effects of xanthium strumarium via PI3K/AKT/mTOR pathway in hepatocellular carcinoma. Evidence-Based Complementary and Alternative Medicine, 2019, 2019: 2176701.

[7] REVATHIDEVI S, MUNIRAJAN AK. Akt in cancer: mediator and more. Seminars in Cancer Biology, 2019, 59: 80–91.

[8] LI A, ZHANG R, ZHANG Y, et al. BEZ235 increases sorafenib inhibition of hepatocellular carcinoma cells by suppressing the PI3K/AKT/mTOR pathway. American Journal of Translational Research, 2019, 11(9): 5573–5585.

[9] PARK SJ, LEE HY, CHOI NR, et al. Calculus Bovis-Fel Uris-Moschus pharmacopuncture's effect on regional cerebral blood flow and mean arterial blood pressure in rats. Journal of Pharmacopuncture, 2013, 16(4): 30–35.

[10] ZHONG XM, REN XC, LOU YL, et al. Effects of *in-vitro* cultured Calculus Bovis on learning and memory impairments of hyperlipemia vascular dementia rats. Journal of Ethnopharmacology, 2016, 192: 390–397.

[11] XIANG D, YANG J, LIU Y, et al. Calculus bovis sativus improves bile acid homeostasis via farnesoid x receptor-mediated signaling in rats with estrogen-induced cholestasis. Frontiers in Pharmacology, 2019, 10: 48.

[12] ZHOU Z, DUN L, WEI B, et al. Musk ketone induces neural stem cell proliferation and differentiation in cerebral ischemia via activation of the PI3K/Akt signaling pathway. Neuroscience, 2020, 435: 1–9.

[13] XU L, CAO Y. Native musk and synthetic musk ketone strongly induced the growth repression and the apoptosis of cancer cells. BMC Complementary and Alternative Medicine, 2016, 16(1): 511.

[14] CARR BI. Hepatic artery chemoembolization for advanced stage HCC: experience of 650 patients. Hepatogastroenterology, 2002, 49(43): 79–86.

[15] DENG Z, XU XY, YUNITA F, et al. Synergistic anti-liver cancer effects of curcumin and total ginsenosides. World Journal of Gastrointestinal Oncology, 2020, 12(10): 1091–1103.

[16] HOU Y, WANG Z, HUANG S, et al. SKA3 Promotes tumor growth by regulating CDK2/P53 phosphorylation in hepatocellular carcinoma. Cell Death & Disease, 2019, 10(12): 929.

[17] GRANDHI MS, KIM AK, RONNEKLEIV-KELLY SM, et al. Hepatocellular carcinoma: from diagnosis to treatment. Surgical Oncology, 2016, 25(2): 74–85.

[18] SUNG H, FERLAY J, SIEGEL RL, et al. Global cancer statistics 2020: GLOBOCAN estimates of incidence and mortality worldwide for 36 cancers 185 countries. CA: a cancer journals for clinicians, 2017, 71(3): 209–249.

[19] FORNER A, REIG M, BRUIX J. Hepatocellular carcinoma. Lancet, 2018, 391(10127): 1301–1314.
[20] BORRELLI A, BONELLI P, TUCCILLO FM, et al. Role of gut microbiota and oxidative stress in the progression of non-alcoholic fatty liver disease to hepatocarcinoma: current and innovative therapeutic approaches. Redox Biology, 2018, 15: 467–479.
[21] JIA W, XIE G, JIA W. Bile acid-microbiota crosstalk in gastrointestinal inflammation and carcinogenesis. Nature Reviews Gastroenterology Hepatology, 2018, 15(2): 111–128.
[22] SINGH V, YEOH BS, CHASSAING B, et al. Dysregulated microbial fermentation of soluble fiber induces cholestatic liver cancer. Cell, 2018, 175(3): 679–694.
[23] CHEN Y, CHEN HN, WANG K, et al. Ketoconazole exacerbates mitophagy to induce apoptosis by downregulating cyclooxygenase-2 in hepatocellular carcinoma. Journal of Hepatology, 2019, 70(1): 66–77.
[24] HE W, XU Y, ZHANG C, et al. Hepatoprotective effect of Calculus Bovis sativus on nonalcoholic fatty liver disease in mice by inhibiting oxidative stress and apoptosis of hepatocytes. Drug Design Development and Therapy, 2017, 11: 3449–3460.
[25] XIANG D, WU T, FENG CY, et al. Upregulation of PDZK1 by Calculus Bovis sativus may play an important role in restoring biliary transport function in intrahepatic cholestasis. Evidence-Based Complementary and Alternative Medicine, 2017, 2017: 1640187.
[26] YU ZJ, XU Y, PENG W, et al. Calculus Bovis: a review of the traditional usages, origin, chemistry, pharmacological activities and toxicology. Journal of Ethnopharmacology, 2020, 254: 112649.
[27] ZHANG Z, ZENG P, GAO W, et al. Exploration of the potential mechanism of Calculus Bovis in treatment of primary liver cancer by network pharmacology. Combinatorial Chemistry & High Throughput Screening, 2021, 24(1): 129–138.
[28] QI W, LI Z, YANG C, et al. Inhibitory mechanism of muscone in liver cancer involves the induction of apoptosis and autophagy. Oncology Reports, 2020, 43(3): 839–850.
[29] GUO Q, XU X, HE S, et al. Xihuang pills enhance the tumor treatment efficacy when combined with chemotherapy: a meta-analysis and systematic review. Journal of Cancer Research and Therapeutics, 2018, 14(Supplement): S1012–S1018.
[30] LI XY, SU L, JIANG YM, et al. The antitumor effect of Xihuang pill on treg cells decreased in tumor microenvironment of 4T1 breast tumor-bearing mice by PI3K/AKT~AP-1 signaling pathway. Evidence-Based Complementary and Alternative Medicine, 2018, 2018: 6714829.
[31] SHAO M, HE Z, YIN Z, et al. Xihuang pill induces apoptosis of human glioblastoma U-87 MG cells via targeting ROS-mediated Akt/mTOR/FOXO1 pathway. Evidence-Based Complementary and Alternative Medicine, 2018, 2018: 6049498.
[32] FU J, ZHU SH, XU HB, et al. Xihuang pill potentiates the anti-tumor effects of temozolomide in glioblastoma xenografts through the Akt/mTOR-dependent pathway. Journal of Ethnopharmacology, 2020, 261: 113071.
[33] FRESNO VARA JA, CASADO E, DE CASTRO J, et al. PI3K/Akt signalling pathway and cancer. Cancer Treatment Reviews, 2004, 30(2): 193–204.
[34] LIEN EC, DIBBLE CC, TOKER A. PI3K signaling in cancer: beyond AKT. Current Opinion in Cell Biology, 2017, 45: 62–71.
[35] SONG M, BODE AM, DONG Z, et al. AKT as a therapeutic target for cancer. Cancer Research, 2019, 79(6): 1019–1031.
[36] JANKU F, YAP TA, MERIC-BERNSTAM F. Targeting the PI3K pathway in cancer: are we making headway. Nature Reviews Clinical Oncology, 2018, 15(5): 273–291.
[37] MOSSMANN D, PARK S, HALL MN. mTOR signalling and cellular metabolism are mutual determinants in cancer. Nature Reviews Cancer, 2018, 18(12): 744–757.
[38] AOKI M, FUJISHITA T. Oncogenic roles of the PI3K/AKT/mTOR axis. Current Topics in Microbiology and Immunology, 2017, 407: 153–189.
[39] ASATI V, MAHAPATRA DK, BHARTI SK. PI3K/Akt/mTOR and Ras/Raf/MEK/ERK signaling pathways inhibitors as anticancer agents: structural and pharmacological perspectives. European Journal of Medicinal Chemistry, 2016, 109: 314–341.
[40] GOLOB-SCHWARZL N, KRASSNIG S, TOEGLHOFER AM, et al. New liver cancer biomarkers: PI3K/AKT/mTOR pathway members and eukaryotic translation initiation factors. European Journal of Cancer, 2017, 83: 56–70.
[41] ALZAHRANI AS. PI3K/Akt/mTOR inhibitors in cancer: at the bench and bedside. Seminars in Cancer Biology, 2019, 59: 125–132.
[42] LI L, LIU JD, GAO GD, et al. Puerarin 6″-O-xyloside suppressed HCC via regulating proliferation, stemness, and apoptosis with inhibited PI3K/AKT/mTOR. Cancer Medicine, 2020, 9(17): 6399–6410.
[43] JIANG S, WANG Q, FENG M, et al. C2-ceramide enhances sorafenib-induced caspase-dependent apoptosis via PI3K/AKT/mTOR and Erk signaling pathways in HCC cells. Applied Microbiology and Biotechnology, 2017, 101(4): 1535–1546.
[44] WU T, DONG X, YU D, et al. Natural product pectolinarigenin inhibits proliferation, induces apoptosis, and causes G2/M phase arrest of HCC via PI3K/AKT/mTOR/ERK signaling pathway. OncoTargets and Therapy, 2018, 11: 8633–8642.
[45] WONG RS. Apoptosis in cancer: from pathogenesis to treatment. Journal of Experimental & Clinical Cancer Research, 2011, 30(1): 87.
[46] MOHAMMAD RM, MUQBIL I, LOWE L, et al. Broad targeting of resistance to apoptosis in cancer. Seminars in Cancer Biology, 2015, 35: S78-S103.
[47] LETAI AG. Diagnosing and exploiting cancer's addiction to blocks in apoptosis. Nature Reviews Cancer, 2008, 8(2): 121–132.

牛黄–麝香联合应用通过 PI3K/AKT/mTOR 信号通路抑制肝癌细胞增殖并诱导其凋亡

宁迪敏[a], 邓哲[a], 吴泳蓉[a], 梅巳[b], 滕永杰[c], 周青[c], 田雪飞[a*]

a. 湖南中医药大学中西医结合学院中药方证转化湖南省重点实验室, 湖南 长沙 410208, 中国
b. 湖南中医药大学生理学教研室, 湖南 长沙 410208, 中国
c. 湖南中医药大学第一附属医院男性病科, 湖南 长沙 410007, 中国

【摘要】目的 探讨牛黄–麝香联合使用对人肝癌细胞 SMMC-7721 及裸鼠肝癌皮下移植瘤的影响，探讨其抗肝癌机制。**方法** 将牛黄–麝香联合应用于体内、体外两种肝癌模型。体外培养人肝癌 SMMC-7721 细胞系，实验分为牛黄–麝香处理组和对照组，采用不同浓度（生药量 0.625、1.25、2.5、5 mg/mL）牛黄–麝香萃取液进行干预，细胞增殖及毒性检测（CCK-8）实验检测肝癌细胞增殖能力，伤口愈合实验检测肝癌细胞迁移能力。制备人肝癌细胞裸鼠皮下移植瘤模型，选择 18 只 5 周龄 SPF 级雄性 BALB/c 裸鼠随机分为模型组（0.9% 生理盐水 0.2 mL/d），牛黄–麝香组 [牛黄 45.5 mg/(kg·d) + 麝香 13 mg/(kg·d)] 与顺铂组（DDP，每周腹腔注射一次 5 mg/kg），每组 6 只，各组裸鼠均给药 14 天。观察裸鼠皮下移植瘤瘤体体积及质量变化，采用实时荧光定量 PCR (RT-PCR) 和蛋白免疫印迹法（Western blot）检测肝癌裸鼠皮下移植瘤模型中磷脂酰肌醇-3-激酶/蛋白激酶 B/哺乳动物雷帕霉素靶蛋白 (PI3K/AKT/mTOR) 通路、凋亡相关因子 p70 S6 Kinase (S6K)、Bax、Bcl-2、caspase-3 和 caspase-9 的表达。原位末端转移酶标记技术（TUNEL）用于凋亡细胞的定量分析。**结果** CCK-8 实验表明，牛黄–麝香联合使用抑制肝癌细胞增殖能力优于使用单味药，且作用效果呈浓度–时间依赖性 ($P < 0.01$)。伤口愈合实验表明，牛黄–麝香联合使用对肝癌细胞迁移能力有明显的抑制作用 ($P < 0.01$)。肝癌裸鼠皮下移植瘤模型实验发现，牛黄–麝香组瘤体体积及质量均低于模型组 ($P < 0.01$)，牛黄–麝香组与 DDP 组 PI3K/AKT/mTOR 信号通路及 S6K 蛋白表达水平均明显下降 ($P < 0.01$)，牛黄–麝香组抑凋亡基因 Bcl-2 的表达下调 ($P < 0.05$)，促凋亡基因 Bax 及凋亡相关因子 caspase-3 和 caspase-9 的表达显著上调 ($P < 0.01$)。TUNEL 实验也进一步证实，二者联用能够促进肝癌细胞凋亡 ($P < 0.01$)。**结论** 牛黄–麝香联合使用能抑制人肝癌细胞 SMMC-7721 的增殖及迁移，并有效抑制肝癌裸鼠皮下移植瘤的生长，其机制可能与下调 PI3K/AKT/mTOR 通路、调控凋亡相关蛋白 caspase-3、caspase-9、Bcl-2 和 Bax 的表达及促进细胞凋亡密切相关。

【关键词】 牛黄；麝香；肝癌细胞；PI3K/AKT/mTOR 信号通路；Caspase-3；Caspase-9；Bcl-2；Bax；细胞凋亡